



Structural, optical, and electrical characterization of spray-deposited $\text{Mg}_{0.02}\text{Zn}_{0.98}\text{Se}$ thin film for buffer layer application

V. S. Ganesha Krishna¹ and M. G. Mahesha^{1,*}

¹Department of Physics, Manipal Institute of Technology, Manipal Academy of Higher Education, 576104 Manipal, India

Received: 27 January 2021

Accepted: 17 June 2021

Published online:
29 June 2021

© The Author(s) 2021

ABSTRACT

In this work, spray-deposited $\text{Mg}_{0.02}\text{Zn}_{0.98}\text{Se}$ thin films were characterized to determine their structural, optical, and electrical properties. The optical band gap of Mg-doped ZnSe thin film was observed to be around 3.05 eV, with high optical transmittance of about 50–70% in the visible region. The crystallite size of Mg-doped ZnSe thin film was about 8 nm, as observed from the X-ray diffraction (XRD) pattern. Elemental composition of Mg-doped ZnSe thin film was confirmed from X-ray energy-dispersive analysis (EDAS). Raman study showed the development of minor strain in ZnSe system due to the incorporation of Mg. The resistivity of the Mg-doped ZnSe film was about 3.82 ohm-m with a carrier concentration of $8.2 \times 10^{11} \text{ cm}^{-3}$. $\text{Mg}_{0.02}\text{Zn}_{0.98}\text{Se}$ thin films exhibited promising opto-electronic properties such as high transparency and conductivity that are essential for a solar buffer layer that could replace relatively toxic CdS layer.

1 Introduction

A characteristic CIGS solar cell comprises a p-CIGS absorber, CdS buffer, and ZnO window layer. The presence of low resistive phases like Cu-Se that forms shunt path is one of the main reasons for the deprived effectiveness of CIGS solar cells [1]. Therefore, a moderately resistive film must be used as a buffer layer. In addition to the toxicity, a lower band gap of CdS results in small spectral response in shorter wavelength or the blue region. Another disadvantage of CdS buffer is the low short circuit current density [2]. Therefore, search for an alternate

material that has the capacity to replace CdS finds importance in CIGS solar cells. Among II-VI compounds, ZnSe thin film with a good optical response, near lattice matching with CIGS, and having a relatively higher band gap than CdS could be the replacement [3]. However, ZnSe film has a relatively lower transmittance [4] and the band gap has to be further tuned to respond in the shorter wavelength region of solar spectra. Mg dopant has the ability to increase both the band gap and transmittance of wide band gap II-VI compounds [5]. Thus, in the present report, Mg-doped ZnSe film is investigated for the possible application as a buffer layer in CIGS solar

Address correspondence to E-mail: mahesha.mg@manipal.edu

cells. Moreover, Mg-doped ZnSe film was prepared by industrially beneficial, cost-effective spray pyrolysis method, adding one more benefit to the list.

2 Experimental details

Mg_{0.02}Zn_{0.98}Se thin films were prepared by spraying the stock solution of 0.05 M magnesium chloride, zinc chloride, and selenourea in water on to glass substrate maintained at 673 ± 5 K. All these chemicals were procured from Sigma Aldrich with research-grade (> 99%) purity. Computerized HOL-MARC spray pyrolysis setup was used for growing the film and the thickness was around 600 nm which was confirmed from BRUKER stylus profilometer. Deposited film was analyzed using X-ray diffractogram recorded using Rigaku Miniflex-600 Cu K α (0.154 nm) with 40 kV, 15 mA at a scan speed of 1°/min and step size of 0.02°. Surface morphology was studied through scanning electron microscopy (SEM) with model Zeiss SEM EVO18. Transmittance spectra were recorded using SHIMADZU UV-1800. Raman spectra were recorded for the film using LabRAM HR (UV) with 325 nm and 514 nm LASER furnished with CCD detector. Hall measurements were carried out using Van der Paw method via computer interfaced Keithley 2450 source meter at room temperature.

3 Results and discussion

X-ray diffraction pattern of Mg_{0.02}Zn_{0.98}Se film is depicted in Fig. 1a. The deposited film had a cubic phase with preferred orientation along (111) plane located at $2\theta = 28.59^\circ$ which matches with the card number 00-005-0522. There was a shift in the peak position for Mg-doped ZnSe thin film from that of pristine (28.28°) [4], showing the successful incorporation of Mg²⁺ ions into Zn²⁺ sites. Crystallite size was estimated using the Scherrer equation [6] and was found to be 8 nm (with the value of Scherrer constant taken as 0.9 assuming the spherical form of crystallites [7]), which is lower than that of ZnSe films [4]. Further discussion on the Scherrer equation could be found elsewhere [7]. Strain and dislocation density in the film were found to be 4.6×10^{-3} and 1.6×10^{16} , respectively. The broadening of XRD peaks could be related to many factors, in which case Williamson–Hall method could be used to reduce the

errors in estimation of the parameters [8, 9]. Crystallite size and strain were estimated using the Williamson–Hall method [8, 9], which takes account of all peaks in the XRD pattern [10]. Crystallite size was estimated from the intercept obtained by linear fitting W–H data points (Fig. 1b). Crystallite size and the average lattice strain were 12 nm, and 6×10^{-3} , respectively. The lattice parameter for the Mg-doped ZnSe sample was 5.4 Å, which is only 3.7% mismatching with that of CIGS indicating MgZnSe thin film as a probable buffer layer.

Phonon behavior of the film was analyzed using the frequency shift of scattered light, i.e., the Raman scattering analysis. For ZnSe, the space group of the cubic unit cell is F43m(T_d²) with four formula units [11]; Primitive cell with one formula, other three are optical branches. With no center of inversion in the unit cell, the transverse optic (TO) and longitudinal optic (LO) modes are Raman active [11, 12]. Raman spectrum for the Mg-doped ZnSe thin film is shown in Fig. 1c. The line shape was fitted using Lorentzian (Fig. 1d) to end up with two deconvoluted peaks at ~ 237 cm⁻¹ and ~ 255 cm⁻¹. The former mode corresponds to $l = 1$, a surface phonon mode observed by Pallavi V Taredesai et al. [13]. The appearance of such surface phonon is a characteristic feature of small particle size [14] that is in line with crystallite size obtained from XRD. The peak at 255 cm⁻¹ corresponds to LO mode of ZnSe. The blue shift in this LO mode compared to the pristine ZnSe thin film [4] is attributed to the compressive strain in the doped film. This is in line with the shift in XRD peak toward higher 2θ .

Scanning electron micrographs showed crackles, pinhole-free, and uniform surface at a magnification of 10k X (Fig. 2a). EDX analysis was done to quantify the amount of constituent elements in the sample. It was found from the EDX spectra (Fig. 2b) that the film had no impurities other than Mg. However, a small amount of oxygen was detected, which could be attributed to the methodology. Composition of Mg, Zn, and Se were 2.10 at%, 57.95 at%, and 39.95 at%, respectively. Se deficiency is majorly from the high-temperature deposition technique, as selenium is more volatile than that of Zn and Mg.

Absorbance (not shown here) for the Mg-doped ZnSe film was recorded from 350 nm to 1100 nm. The corresponding transmittance plot is shown in Fig. 2c. The transmittance of the Mg-doped film ($\sim 60\%$) nearly doubled compared to the pristine ZnSe sample

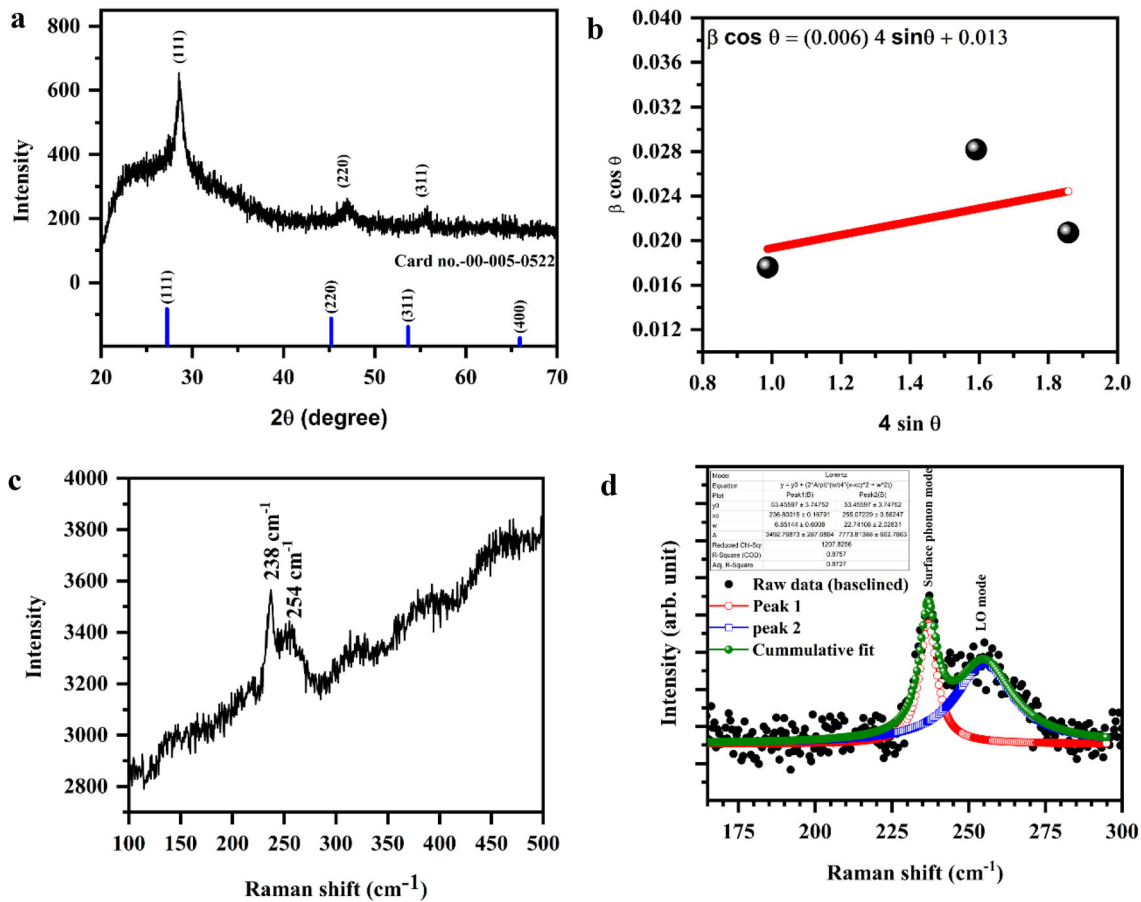


Fig. 1 a XRD pattern of Mg-doped ZnSe thin film, b Williamson–Hall plot for average crystallite size and lattice strain, c Raman spectra of Mg-doped ZnSe thin film, d Lorentzian peak fit of Raman spectra

($\sim 30\%$) [4] in the visible region. Tauc plot of $(\alpha h\nu)^2$ vs. $h\nu$ as shown in Fig. 2a was used to find band gap, where α is the absorption coefficient, h is the plank’s constant, ν is the frequency. The curve in the plot was observed to be linear with the power of $(\alpha h\nu)$ as 2 against $h\nu$, indicating the direct band gap [15, 16]. From the intercept of the linear curve, the band gap was estimated. The band gap of Mg-doped film was found to be 3.05 eV from this Tauc plot [17]. This value is higher than the band gap observed for the ZnSe sample (2.73 eV) [4]. This high band gap will enable blue or shorter wavelength light photons to reach the CIGS absorber, wherein this feature is completely absent in CdS and ZnSe buffer layers. Degree of randomness and defect states were found by calculating the Urbach tail, which was obtained by taking the reciprocal of the slope of $\ln \alpha$ vs. $h\nu$ plot (inset of Fig. 2c), where α is the absorption coefficient and $h\nu$ is the photon energy [18]. Urbach energy in the film was found to be 276 meV. Urbach tail

quantified using a parameter called NEAR [19] was 0.88, indicating the presence of defect states [20]. The refractive index was calculated from the Herve-Vandamme relation [21] and found to be 2.33. Thus, with optimum band gap and refractive index, Mg-doped ZnSe becomes one of the competing candidates for buffer layer along with other materials.

To determine the electrical parameters for the deposited films, the Van der Paw method was adopted. A carrier density of $8.2 \times 10^{11} \text{ cm}^{-3}$, a resistivity of 3.82 ohm-m, and mobility of $2 \text{ m}^2/\text{V/s}$ were observed. The carrier density and resistivity were lower than the CdS films reported by Friedlmeier et al. [22], showing the optimum electrical characteristics of Mg-doped ZnSe films for the buffer layer. All the parameters obtained for the deposited film are listed in Table 1.

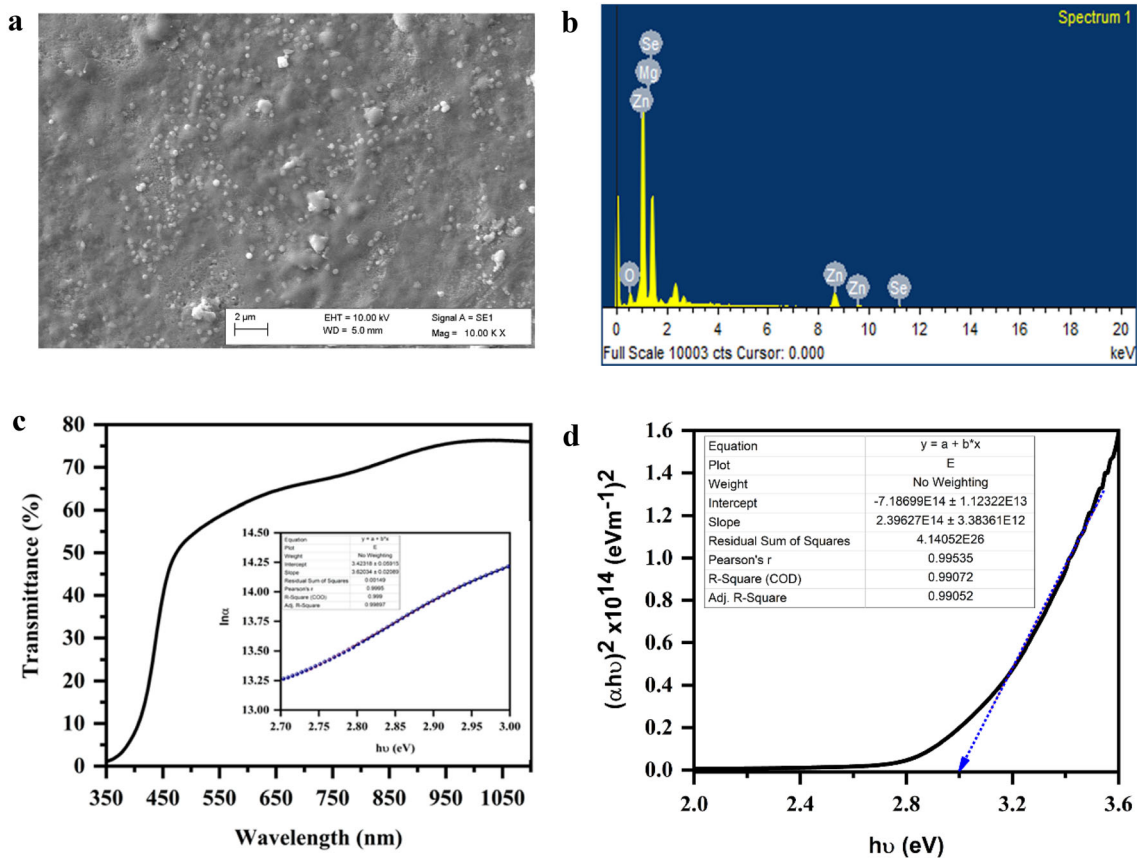


Fig. 2 **a** Scanning electron micrograph, **b** EDX spectra of MgZnSe thin film, **c** transmittance spectra (inset, urbach plot), **d** Tauc plot for $\text{Mg}_{0.02}\text{Zn}_{0.98}\text{Se}$ thin film

4 Conclusion

ZnSe film doped with magnesium was deposited using spray pyrolysis and characterized for structural, optical, and electrical properties as a buffer

Table 1 Structural, optical, and electrical parameters for $\text{Mg}_{0.02}\text{Zn}_{0.98}\text{Se}$ thin films

Crystallite size (Scherrer)	8 nm
Crystallite size (W-H plot)	12 nm
Lattice parameter	5.4 Å
Strain (Scherrer)	4.6×10^{-3}
Strain (W-H plot)	6.0×10^{-3}
Dislocation density	$1.6 \times 10^{16} / \text{m}^2$
Band gap	3.05 eV
Urbach energy	276 meV
NEAR	0.88
Refractive index	2.33
Resistivity	3.82 ohm-m
Mobility	$2 \text{ m}^2/\text{V/s}$

layer in CIGS. Crystallite size was found to be 8 nm with a lower strain of 4.6×10^{-3} using the Scherrer equation and 12 nm, 6×10^{-3} using the W–H method. Mg-doped ZnSe film had an optimum band gap of 3.05 eV for buffer layer application. A high carrier density of $8.2 \times 10^{11} \text{ cm}^{-3}$, a resistivity of 3.82 ohm-m, and mobility of $2 \text{ m}^2/\text{V/s}$ were observed. Having a lattice parameter closer to that of CIGS with only 3.7% of mismatch, and a wide band gap of 3.05 eV, it can be used as a buffer layer in CIGS solar cells to replace toxic CdS.

Acknowledgements

This manuscript is part of the special issue of selected papers from the 6th edition of biennial International Conference on Nanoscience and Nanotechnology (ICONN-2021). Ganesha Krishna V S is thankful to DST India for providing INSPIRE fellowship through grant number IF190268.

Authors' contributions

VSGK contributed to the investigation, formal analysis, methodology, visualization, writing of the original draft. MMG contributed to the conceptualization, supervision, writing, reviewing and editing of the manuscript.

Funding

Open access funding provided by Manipal Academy of Higher Education, Manipal.

Data availability

Data will be made available on request.

Declarations

Conflict of interest The authors declare that they have no known competing financial interests or personal relationships that could have appeared to influence the work reported in this paper.

Open Access This article is licensed under a Creative Commons Attribution 4.0 International License, which permits use, sharing, adaptation, distribution and reproduction in any medium or format, as long as you give appropriate credit to the original author(s) and the source, provide a link to the Creative Commons licence, and indicate if changes were made. The images or other third party material in this article are included in the article's Creative Commons licence, unless indicated otherwise in a credit line to the material. If material is not included in the article's Creative Commons licence and your intended use is not permitted by statutory regulation or exceeds the permitted use, you will need to obtain permission directly from the copyright holder. To view a copy of this licence, visit <http://creativecommons.org/licenses/by/4.0/>.

References

1. Y. Ohtake, K. Kushiya, M. Ichikawa, *Jpn. J. Appl. Phys.* **34**, 5949 (1995)
2. K. Orgassa, U. Rau, Q. Nguyen, H.W. Schock, *Prog. Photovoltaics Res. Appl.* **10**, 457 (2002)
3. E. Bacaksiz, S. Aksu, I. Polat, S. Yilmaz, M. Altunbas, *J. Alloys Compd.* **487**, 280 (2009)
4. G. Krishna, M. Mahesha, *Surfaces and Interfaces* **20**, 100509 (2020)
5. G. Krishna, V.S., P.S. Patil, S.R. Maidur, Mahesha, *Opt. Mater. (Amst)*. **96**, 109304 (2019)
6. B.D. Cullity (1978) *Elements of X-Ray Diffraction* (Addison Wesley Publishing company)
7. V. Uvarov, I. Popov, *Mater. Charact.* **85**, 111 (2013)
8. K.A. Aly, N.M. Khalil, Y. Algamal, Q.M.A. Saleem, *Mater. Chem. Phys.* **193**, 182 (2017)
9. G.K. Williamson, W.H. Hall, *Acta Metall.* **1**, 22 (1953)
10. S.K. Abdel-Aal, A.S. Abdel-Rahman, *J. Nanoparticle Res.* **22**, 267 (2020)
11. L. Sun, L. Shi, C. Wang (2016) *Appl. Mol. Spectrosc. to Curr. Res. Chem. Biol. Sci.*
12. S.K. Abdel-Aal, A.S. Abdel-Rahman, W.M. Gamal, M. Abdel-Kader, H.S. Ayoub, A.F. El-Sherif, M.F. Kandeel, S. Bozhko, E.E. Yakimov, E.B. Yakimov, *Acta Crystallogr. Sect. B Struct. Sci. Cryst. Eng. Mater.* **75**, 880 (2019)
13. P.V. Teredesai, F.L. Deepak, A. Govindaraj, A.K. Sood, C.N.R. Rao, *J. Nanosci. Nanotechnol.* **2**, 495 (2002)
14. C.X. Shan, Z. Liu, X.T. Zhang, C.C. Wong, S.K. Hark, *Nanotechnology* **17**, 5561 (2006)
15. I.S. Y. IM. El, T.A. Radaf, Hamid, *Mater. Res. Express* **5**, 25 (2018)
16. S.K. Abdel-Aal, A.S. Abdel-Rahman, *J. Electron. Mater.* **48**, 1686 (2019)
17. J. Tauc, R. Grigorovici, A. Vancu, *Phys. Status Solidi Basic Res.* **15**, 627 (1966)
18. F. Urbach, *Phys. Rev.* **92**, 1324 (1953)
19. B.D. Viezbicke, S. Patel, B.E. Davis, D.P. Birnie, *Phys. Status Solidi Basic Res.* **252**, 1700 (2015)
20. V.S. Ganesha Krishna, M.G. Mahesha, *J. Alloys Compd.* **848**, 156568 (2020)
21. L.K.J.V.P. HERVE, *Infrared Phys. Technol.* **35**, 609 (1994)
22. T.M. Friedlmeier, P. Jackson, A. Bauer, D. Hariskos, O. Kiowski, R. Wuerz, M. Powalla, *J. Photovoltaics* **5**, 1487 (2015)

Publisher's Note Springer Nature remains neutral with regard to jurisdictional claims in published maps and institutional affiliations.